ACS APPLIED MATERIALS & INTERFACES

Research Article

www.acsami.org

Interferometry Study of Aqueous Lubrication on the Surface of Polyelectrolyte Brush

Motoyasu Kobayashi,[†] Hiroyoshi Tanaka,[‡,§] Myo Minn,[†,§] Joichi Sugimura,[‡,§] and Atsushi Takahara*[,†,§,⊥]

[†]Japan Science and Technology Agency (JST) ERATO Takahara Soft Interfaces Project, CE80, Kyushu University, 744 Motooka, Nishi-ku, Fukuoka 819-0395, Japan

[‡]Graduate School of Engineering, Kyushu University, 744 Motooka, Nishi-ku, Fukuoka 819-0395, Japan

[§]WPI International Institute for Carbon-Neutral Energy Research (WPI-I2CNER), Kyushu University, 744 Motooka, Nishi-ku, Fukuoka 819-0395, Japan

[⊥]Institute for Materials Chemistry and Engineering, Kyushu University, 744 Motooka, Nishi-ku, Fukuoka 819-0395, Japan

ABSTRACT: The water lubrication behavior of a polyelectrolyte brush was investigated by using double-spacer-layer ultra-thin-film interferometry to determine the thickness of the aqueous lubrication layer present at the interface between the brush and a spherical glass lens. A hydrophilic poly{[2-(methacryloyloxy)ethyl]trimethylammonium chloride} brush was prepared on an optical glass disk coated with layers of semireflective chromium and silica. The thickness of the hydrodynamic lubrication layer was estimated interferometrically. On increasing the sliding velocity from 10^{-5} to 10^{-1} m·s^{-1}, the gap between the rotating disk and loading sphere glass lens showed a marked increase to 130 nm at 2×10^{-2} m·s^{-1}, and the friction coefficient simultaneously decreased to 0.01−0.02, indicating that the polyelectrolyte brush promoted the formation of a fluid lubrication layer that separates the rubbing surfaces, preventing direct contact and providing a low friction coefficient.

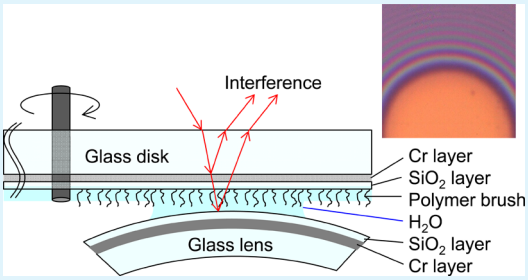

KEYWORDS: *water lubrication, polymer brush, interferometry, polyelectrolyte, friction, elastohydrodynamic lubrication*

INTRODUCTION

A reduction in the friction coefficient of a surface with tethered hydrophilic polymers or polyelectrolytes under wet conditions has been widely demonstrated by experiment and confirmed theoretically. Surface-tethered polymers of sufficient graft density are referred to as polymer brushes[1,2] and exhibit unique tribological properties in suitable solvents.[3] In principle, densely grafted polymer chains in a good solvent are stretched away from the surface to reduce their mutual interactions and to avoid overlapping other chains. The state of chain stretching is determined by the balance between the osmotic pressure arising from the high concentration of polymer and the elastic restoring force of the polymer chain. When two polymer brush-covered surfaces are brought into contact in a good solvent, they normally repel one another because of the excluded-volume effect of the polymer segments; this can suppress mutual interpenetration of the two compressed brushes. This is the classical mechanism for efficient lubrication of solvated polymer brushes based on repulsive steric forces.[4] By using a surface-force balance, Klein et al. showed experimentally that polyelectrolyte brushes can act as efficient lubricants between mica surfaces in aqueous solutions.[5−8] Recently, Tsujii et al. showed that high-density (concentrated) brushes of poly(methyl methacrylate) in toluene can have extremely low friction coefficients.[9]

In the case of polyelectrolyte brushes in aqueous media, the osmotic pressure of the free counterions within the charged brush also contributes to an extremely low friction property.[10−12] The hydration layer bound to the charged sites and the fluidity of the hydrating water also play important roles in boundary lubrication.[13,14] The lubrication properties of polyelectrolyte brushes are affected by many factors, such as the graft density,[15−17] ionic strength,[18] solvent quality,[19,20] and Coulombic repulsive and attractive interactions of polar functional groups,[21,22] which can be directly measured by using a surface-force balance[23,24] or atomic force microscopy (AFM).[25] Superhydrophilic polymer brushes as low-friction boundary layers in water lubrication systems would therefore be expected to show extremely low coefficients of friction.[26−28]

Takahara and co-workers investigated the macroscopic tribological characteristics of ionic[29−31] and nonionic[32,33] polymer brushes in water. In particular, they examined the dependence of the friction coefficient on the friction velocity in the range 10^{-5} to 10^{-1} m·s^{-1} by using a conventional ball-on-plate reciprocating tribotester with a glass ball probe sliding on the substrate under a normal load of 0.49 N at 298 K.[34,35] They found that a significant reduction in the friction coefficient of a polymer brush in water occurred at friction velocities of more than 10^{-2} m·s^{-1}. For example, the friction coefficients of poly{[2-(methacryloyloxy)ethyl]trimethylammonium chloride}

Received: August 31, 2014
Accepted: October 23, 2014
Published: October 23, 2014

(PMTAC) brushes in water were 0.1−0.2 at slower friction velocities of 10^{-5} to 10^{-3} m·s^{-1}, whereas the friction coefficient fell to 0.01−0.03 at friction velocities above 10^{-2} to 10^{-3} m·s^{-1}, despite the high normal pressure of approximately 139 MPa on the contact area, as estimated by means of Hertz's contact mechanics theory. This normal pressure is much higher than the osmotic pressure associated with the swollen brush in the solution.

It has been shown experimentally that, in general, the friction coefficients in lubrication systems are markedly affected by the sliding velocity, the viscosity of the lubricating fluid, and the normal pressure. The dependence of the friction on these factors is well described by the Stribeck curve.[36] When two surfaces come into contact and slide over one another in an oil at a low sliding velocity, boundary lubrication occurs, inducing a high coefficient of friction, whereas fluid lubrication takes place at faster sliding velocities, resulting in a significant reduction in friction because a very thin film of oil is generated that separates the rubbing surfaces, preventing direct contact and wear. Lubrication that is dominated by such elastohydrodynamic effects is referred to as elastohydrodynamic lubrication (EHL).[37] In contrast, water cannot form a stable lubrication layer at the friction interface at low sliding velocities because of its low viscosity in comparison with oil. In biological interfaces, such as synovial joints, this disadvantage is overcome by the use of glycoproteins or superhydrophilic ionic polymers as viscosity improvers that have suitable viscoelastic properties in solution and induce the formation of an EHL layer. The formation of an EHL layer by artificial hydrophilic polymer brushes in water at relatively slow sliding velocities to afford a reduction in the friction coefficient is therefore an interesting phenomenon. Furthermore, the transition of the lubrication mode for hydrophilic polymer brushes occurs at a sliding velocity of 10^{-2} m·s^{-1}, which is slower than the corresponding velocity for conventional oil-based lubrication.[38]

We began our attempts to make direct observations of the water-lubrication layer on brush surfaces by an in situ observation method: interferometry. Optical interferometry has been frequently used to measure the thickness of EHL films between lubricated solid surfaces.[39−41] The typical apparatus consists of a ball-on-disk setup, consisting of a loaded steel ball and transparent flat glass (or sapphire) disk covered with a semireflective layer of chromium (Cr). In our current work, an additional layer of silica was deposited on top of the thin Cr layer to form a double spacer layer that reduced wear during sliding and could also be used as a substrate on which to bind initiating functional groups for subsequent surface-initiated atom transfer radical polymerization (SI-ATRP) to fabricate a polyelectrolyte brush (Figure 1). We showed that double-spacer-layer ultra-thin-film interferometry can be used to measure the thickness of the aqueous lubrication layer at the interface of the polyelectrolyte brush and a sphere glass lens.

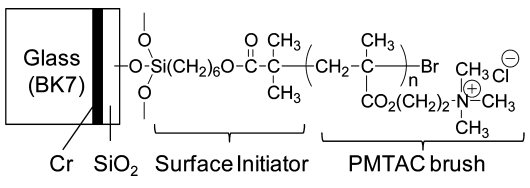

Figure 1. Chemical structure of the PMTAC brush on an optical glass disk (BK7) coated with layers of Cr and SiO_2. A similar surface-initiator layer and PMTAC brush were also prepared on a silicon wafer.

EXPERIMENTAL SECTION

Materials. Copper(I) bromide (CuBr, 99.9%; Wako Pure Chemical Industries Ltd., Osaka) was purified by successive washing with acetic acid and ethanol then dried under vacuum. Ethyl 2-bromoisobutyrate (EB, Tokyo Chemical Inc., 98%) was dried and distilled over CaH_2 before use. 2,2′-Bipyridyl (bpy, 99.5%; Wako), and 2,2,2-trifluoroethanol (TFE, 99.9%; Acros Organics, Geel), were used without further purification. An aqueous solution of 2-[(methacryloyloxy)ethyl] trimethylammonium chloride (MTAC) (Sigma-Aldrich Corp, St. Louis, MO) was concentrated by using a vacuum pump to remove water, and the residue was dissolved in TFE. The TFE solution of MTAC was purified by sequential column chromatography on alumina and filtered through a membrane filter. One surface each of an optical-glass disk (diameter = 80 mm, thickness = 8 mm; BK7; Sigma Koki, Toykyo) and an optical-glass lens (radius of curvature 10.38 mm; Sigma Koki) were coated successively with layers of chromium and silica by sputter deposition under reduced pressure by using a radio frequency (RF) sputtering instrument. The chromium layer of 150 nm thickness was prepared on a BK 7 disk at 200 °C for 3 s under the argon working gas pressure at 0.2 Pa and 200 W of sputter power. The silica coating layer of 150 nm thickness was prepared on the Cr-coated BK 7 disk at 100 °C for 14 min for 30 s under the argon pressure at 0.2 Pa and 100 W of putter power. 6′-(Triethoxysilyl)hexyl 2-bromo-2-methylpropanoate (BHE) was synthesized as described previously.[33] Monolayers of BHE were deposited on the Cr−SiO_2-coated glass disk (Figure 1) and on a silicon wafer by chemical vapor deposition. Deionized water was purified by using a NanoPure Water system (Millipore Inc., Billerica, MA).

Preparation of Polymer Brushes by SI-ATRP.[45] The coated glass disk or silicon wafer was placed in a well-dried flask fitted with a stopcock, and a 2.0 M solution of MTAC in TFE (39.6 mL), and *i*-PrOH were added. The solution was degassed by three freeze−thaw cycles. CuBr (0.103 mmol) and bpy (0.200 mmol) were introduced into a separate glass tube and degassed by seven cycles of vacuum pumping and flushing with argon. A solution of the free initiator EB (0.0106 mmol) diluted with TFE (0.20 M) was added to the CuBr/bpy catalyst solution and immediately gave a homogeneous solution with a characteristic red color. This copper catalyst solution was degassed by repeated freeze−thaw cycles and then injected into the MTAC monomer solution. The resulting mixture was degassed once more by repeated freeze−thaw cycles to remove any oxygen and then stirred in an oil bath at 333 K for 24 h under argon to generate a PMTAC brush from the substrates and free (unbound) PMTAC from the EB. The reaction was stopped by opening the glass vessel to allow air to enter at 273 K. The reaction mixture was then poured into tetrahydrofuran (THF) to precipitate free polymer and any unreacted MTAC. The silicon wafer was washed with TFE in a Soxhlet apparatus for 12 h to remove free polymer adsorbed on its surface, and then dried under reduced pressure. The chemical structure of the resulting brush on the glass disk is shown in Figure 1.

Characterization. The number-average molecular weight (M_n) and molecular-weight dispersity (MWD) of the free soluble PMTAC were determined by size-exclusion chromatography (SEC) using a Shimadzu HPLC system connected to one Tosho G3000PW_{XL}-CP and two G5000PW_{XL}-CP polystyrene gel columns. The SEC system was equipped with a multiangle light-scattering detector (MALS; Wyatt Technology Corp., Santa Barbara, CA), a 30 mW GaAs linearly polarized laser with wavelength λ = 690 nm (DAWN-EOS; Wyatt Technology), and reflective index detector (Shimadzu RID-10A). The columns were eluted with 500 mM aqueous acetic acid containing sodium nitrate (200 mM) at a rate of 0.6 mL·min^{-1}.

Friction Tests. Friction tests were performed on a Tribostation Type 32 machine (Shinto Scientific Co., Ltd., Tokyo, Japan) by sliding a 10 mm diameter glass ball on the substrates for a distance of 20 mm at a sliding velocity of 10^{-5} to 10^{-1} m·s^{-1} at 298 K. The frictional forces on the polymer brushes were measured by using a strain gauge

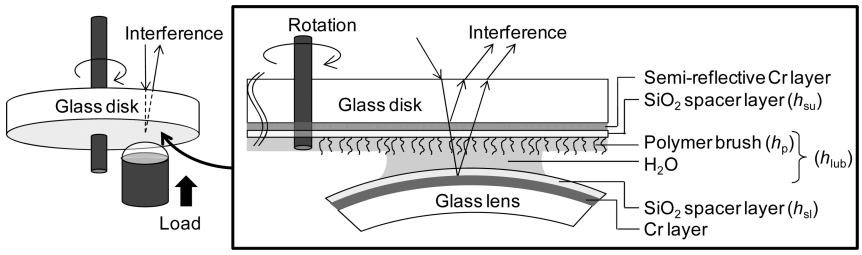

Figure 2. Schematic view of the interferometry method using a ball-on-disk configuration. The glass disk and lens were made of optical glass (BK7). The surfaces of the glass disk and lens were sequentially coated with chromium and silica layers by sputter deposition under reduced pressure.

and recorded on a computer. The normal load was controlled by placing a dead weight (0.49 N) on top of the holder for the glass ball. The normal pressure was estimated to be 139 MPa by means of the Hertz contact theory.[43] The setup of the friction tester has been described in a previous paper.[32]

Double-Spacer-Layer Ultra-Thin-Film Interferometry. A transparent optical glass (BK7) disk (80 × 8 mm) and a glass lens (curvature radius = 10.38 mm) coated with layers of Cr and a silica were prepared as describe above. The surface of the flat glass disk was modified with a PMTAC brush. Figure 2 shows the white-light interferometry setup for measuring the thickness of the lubricating film and the spacer layer. The glass lens was loaded against the flat transparent disk with water sandwiched between them, and a layer of lubricant formed when the glass lens and the disc were rotated. When a coaxial beam of white light was shone onto the contact area between the lens and disk, Fizeau interference fringes were generated by light reflecting from either side of the gap between the disk and the glass lens. The interference fringes were magnified by a microscope and captured by a video device.

In the interference fringes, the maximum intensity occurs at λ_d, according to eq 1

$$2\{(h_{su} + h_{sl})n_s + h_{lub}n_{lub}\} = (N - \phi)\lambda_d \quad (1)$$

where h_{su} and h_{sl} are the thicknesses of the SiO_2 spacer layers on the disk and on the lens, respectively, h_{lub} is the thickness of the lubrication layer, and n_s and n_{lub} are the refractive indices of the spacer layer and lubricant layer, respectively. N (N = 1, 2, 3, ...) is the fringe order, and ϕ is the initial phase change. The thickness of the silica layer was approximately 300 nm ($h_{su} + h_{sl}$ = 300 nm). By using the thickness (h_p) and refractive index (n_p) of a compressed polymer brush in the static contact state, the thicknesses h_{su} and h_{sl} were determined means of eq 2

$$2(h_{su} + h_{sl})n_s + 2h_pn_p = (N - \phi)\lambda_{static} \quad (2)$$

where λ_{static} is the wavelength at which the maximum intensity occurs in the static contact state.

The thickness of the lubrication layer containing the brush and water was calculated from the Hue value (Hue saturation − brightness numbers), and the intensity values from the digitized color interferogram images (512 × 512 pixels). Figure 3a shows the Hue value converted into a color interferogram from the center of the contact area to the outer fringes. The gap between the disk and lens along with radius direction can be estimated by means of Hertz contact theory (Figure 3b) for a plane−sphere contact mode.[40]

In this study, we calculated the thickness of the lubricating film directly from the interference color, rather than from light wavelength, by using the spacer layer imaging method (SLIM).[41] The relationship between the Hue value and the gap was obtained from Figure 3 and described by fitting it to a polynomial function. The gap between the opposing silicon spacer layers was determined from several Hue calibration curves with various level functions.

RESULTS AND DISCUSSION

SI-ATRP of MTAC was carried out in the presence of BHE immobilized on a Cr−SiO_2-coated glass disk and a silicon wafer

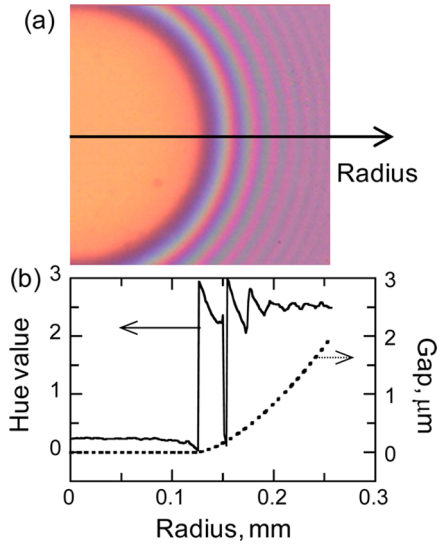

Figure 3. (a) Static interferogram and (b) the Hue value (solid line) and the corresponding gap (dotted line) calculated from Hertz contact theory.

to give PMTAC brushes on the glass disk and the Si wafer; simultaneously, polymerization by sacrificial free EB initiator gave unbound free PMTAC in solution. The M_n of the unbound PMTAC generated at the same time as the brush was determined by SEC to be 738 000 g mol^{-1}. The dry thickness of a PMTAC brush on a silicon wafer under air was measured by ellipsometry to be 170 nm. Although we were unable to measure the thickness of the brush on the Cr−SiO_2-coated glass disk directly in the current study, its dry thickness on the glass disk would be expected to be similar to that on the silicon wafer. The roughness of the dry brush surface and the Cr−SiO_2-coated glass disk could not be estimated by AFM because sample stage width of AFM was much smaller than glass disk. We observed the root-mean-square (rms) value of roughness of the brush surface on Si wafer, which was simultaneously prepared with brush on the glass disk, to be 2.1 ± 0.5 nm in 10 × 10 μm^2 measured by AFM. We supposed that the roughness of Cr-SiO_2-coated glass disk would be slightly (approximately 1−2 nm) larger than Si wafers, but would be similar level to the roughness of the brush. Therefore, we supposed that the brush surface on the Cr-SiO_2-coated glass disk would be expected to have a similar rms value to that on the Si wafer.

Water smoothly spread over the surface of the glass disk with the PMTAC brush. The wet disk was mounted on a rotating holder and contacted with the spherical glass lens under a load of 2.8 N. The theoretical normal pressure, based on Hertzian contact, was 139 MPa. An interferometric image was recorded in the static state (Figure 3) to determine the thickness of the

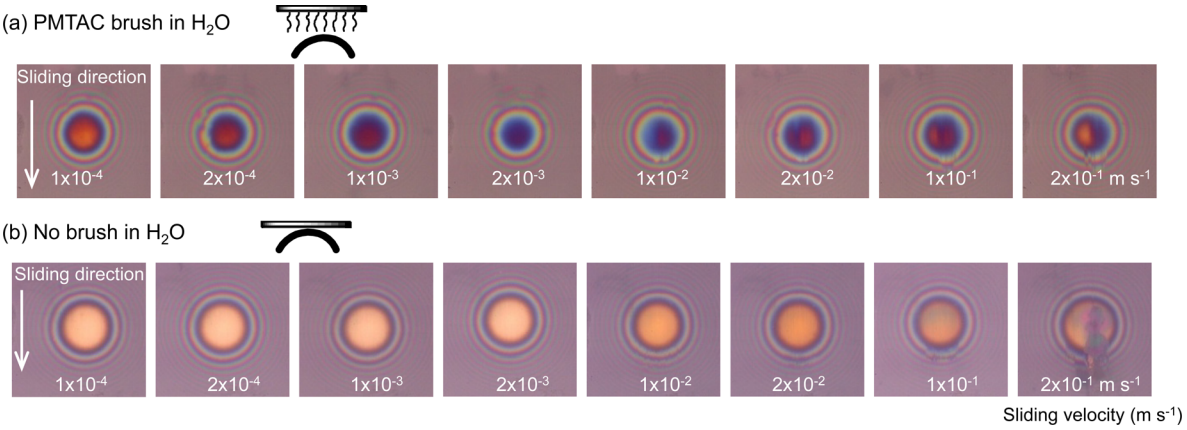

Figure 4. Captured interferometric images of (a) the PMTAC brush, (b) the glass disk and lens in water under a load of 130 MPa at various sliding velocities in the range 1×10^{-4} to 2×10^{-1} m·s^{-1} at 298 K.

gap between the glass disk and glass lens on the basis of the Hue values, as described in the Experimental Section.

Interferometric images of the PMTAC brush in water at various sliding velocities are shown in Figure 4a. During each run of friction testing, the sliding velocity was changed in a stepwise manner from 1×10^{-4} to 2×10^{-1} m·s^{-1}, without stopping the rotation. Interferometric images were recorded continuously by a video camera. The photographs in Figure 4 show typical colors observed during sliding at various sliding velocities. The brightest area in the circle is the contact area between the brush surface and the sliding glass sphere probe. On increasing the sliding velocity from 1×10^{-4} to 2×10^{-2} m·s^{-1}, the interference color changed from orange to blue, indicating an increase in the gap between the glass plate and the spherical glass lens. At a velocity of 2×10^{-2} m·s^{-1}, the orange color partially reappeared, but a blue area also remained.

Figure 5 represent the gap between the brush substrate and glass lens calculated from the Hue value. The interference

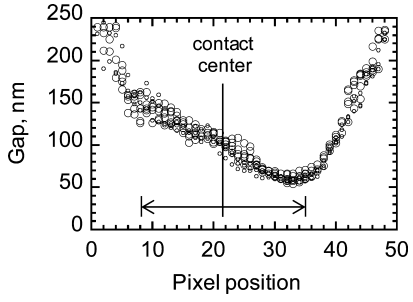

Figure 5. Gap profile calculated from digitized pixel color in the contact area between the lens and glass disk bearing PMTAC brush at a sliding velocity of 1×10^{-2} m·s^{-1} at 298 K. See also the color image in Figure 4a.

occurred between light reflected from the semireflective Cr layer of the glass disk and light reflected from the Cr layer of the glass lens; therefore, the interference color is related to the distance between these two Cr layers, i.e., h_{su}, h_{sl}, and, in particular, h_{lub}, as described in eq 1.

Let us now examine the relationship between the gap in Figure 5 and h_{lub}. In our experiment, the gap was regarded as being zero when the brush contacted the glass lens in the static state. The brush would have been significantly compressed under the load of the glass lens in the static state. The value of h_{lub} in the static state is therefore the thickness of the compressed brush layer, which was approximately 170 nm. Therefore, the gap in Figure 5 is greater than h_{lub} as a result of an additional thickness caused by the sliding.

In Figure 6, the square symbols represent the sliding velocity dependence of the gap. The gap and the error bar are the

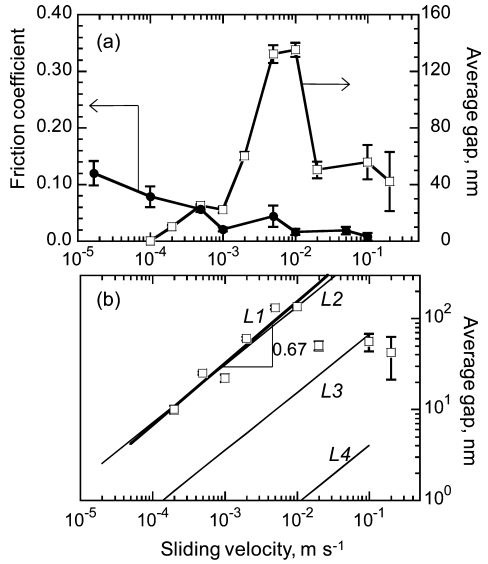

Figure 6. (a) Dependence of the friction coefficient (filled circles) on the sliding velocity for a PMTAC brush in water, measured by using a linearly reciprocating tribotester with a 10 mm-diameter glass ball sliding over a distance of 20 mm under a load of 0.49 N, and the average gap (open squares) calculated by interferometry using a ball-on-disk configuration in the range 1×10^{-4} to 2×10^{-1} m·s^{-1} at 298 K. (b) Double logarithmic plot of the average gap versus the sliding velocity. The solid bold line ($L1$) has a slope of 0.67. The solid narrow lines ($L2$, $L3$, and $L4$) are the calculated thicknesses of hydrodynamic lubrication layers for 40, 15, and 0 wt % PMTAC aqueous solutions, respectively.

average value and standard deviation calculated from the pixel color in the area of contact center between the lens and glass disk. Typical gap profile near the contact center is shown in Figure 5. On increasing the sliding velocity, as shown in Figure 6a, the gap increased significantly up to a value of 130 nm at a velocity of 10^{-2} m·s^{-1}, indicating that the opposing SiO_2 spacer layers on the disk and lens were separated by 300 nm. At

dx.doi.org/10.1021/am505906h | ACS Appl. Mater. Interfaces 2014, 6, 20365−20371

velocities much faster than 10^{-2} m·s^{-1}, an orange color was partially observed again; however, a 50 nm thick lubrication layer remained in a circle area throughout the friction tests.

The circle symbols in Figure 6a indicate the friction coefficients for a PMTAC brush on a silicon wafer in water measured at various velocities by using a reciprocating tribotester with a glass ball probe under a load of 139 MPa. Because the interferometry apparatus could not measure the frictional force, the friction coefficient was independently measured by using a ball-on-plate tribotester under similar conditions of friction to those in the ball-on-disk interferometry system. The friction coefficient in water was 0.12 at 10^{-5} m·s^{-1} and began to decrease significantly at 10^{-3} m·s^{-1}, eventually reaching 0.02. At this friction velocity, the apparent gap also began to increase from 30 to 100 nm. This marked reduction in the friction coefficient at a certain velocity might be caused by a change in the friction mode. At low sliding velocities, interactions between the brush and friction probe dominate the friction and give rise to a large friction coefficient (boundary or interfacial friction). On increasing the sliding velocity, a hydrodynamic lubrication layer is formed that separates the sliding surfaces and reduces the friction force. It is generally known that the friction coefficient in a hydrodynamic lubrication state increases gradually with the friction velocity as a result of fluid resistance. However, no such increase in the friction coefficient was observed in the range 10^{-3} to 10^{-1} m·s^{-1} in the current experiments. By analogy to the Stribeck curve, the effect of fluid resistance should appear at sliding velocities much larger than 1 m·s^{-1}. The relationship between the thickness of the lubricating layer and the velocity, as shown in Figure 6b, will be discussed later.

Although the gap between the disk and lens decreased to 50 nm at 10^{-1} m·s^{-1}, the friction coefficient in water was still as low as 0.01−0.02. In addition, two different colored regions were observed in the contact circle area of the interferometry image (Figure 4a), indicating variations in the thickness of the lubrication layer. We therefore assumed that the PMTAC brush was in a mixed lubrication state at velocities of 10^{-3} to 10^{-1} m·s^{-1}.

The increase of the gap and the reduction in friction coefficient at 10^{-3} m·s^{-1} were reproducible phenomenon when increasing the sliding velocity. The measurement with decreasing sliding velocity from faster to lower rate have not been tried in this study.

On the other hand, no significant color change was observed in the interferometry images of the glass disk without a brush in water in the range $1 \times 10^{-4} - 1 \times 10^{-1}$ m·s^{-1}, as shown in Figure 4b. Figure 7 shows that the friction coefficient of glass was as high as 0.2 at 1×10^{-4} to 1×10^{-2} m·s^{-1}, and the gap between glass disk and lens was almost zero. Therefore, no lubrication layer was formed between the bare glass surfaces at slow sliding velocities, even under wet conditions. When the sliding velocity reached a value in excess of 1×10^{-1} m·s^{-1}, the friction coefficient decreased to 0.1 and the gap simultaneously increased to 15 nm, probably due to a transition from boundary lubrication to a mixed lubrication mode.

One significant difference between the brush-modified disk and the bare glass disk was in the wear track. The brush-modified disk showed no major damage due wear, even after ball-on-disk friction testing in water, whereas a wear track was clearly observed on the surface of the bare disk. As shown in Figure 4b, the ring-shaped interferometric image of the bare glass disk collapsed at a sliding velocity of 2×10^{-1} m·s^{-1} as a result of wear and the formation of wear debris. Although the wear was not quantified in the current study, it would be necessary in the future work.

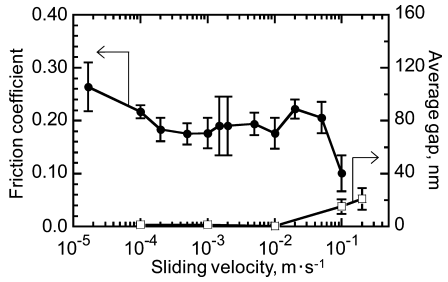

Figure 7. Sliding velocity dependence of the friction coefficient (filled circles) of a glass plate without a brush in water measured by using a linear-reciprocating tribotester with a glass ball (10 mm diameter) sliding over a distance of 20 mm under a load of 0.49 N, and the average gap (open squares) calculated by the interferometry (Figure 4b) using a ball-on-disk configuration in the range of 1×10^{-4} to 2×10^{-1} m·s^{-1} at 298 K.

It is widely accepted that the central thickness of an EHL layer increases with the 0.67 power of the sliding velocity and the lubricant viscosity.[45] As shown in Figure 6b, a double logarithmic plot of the average gap near the center of the contact circle showed a proportional relationship at sliding velocities in the range 10^{-4} to 10^{-2} m·s^{-1}, the slope of which was well agreed with 0.67 [bold line *L*1 in Figure 6b]. This result indicated that the swollen polyelectrolyte brush in water promoted hydrodynamic lubrication. At sliding velocities much greater than 2×10^{-2} m·s^{-1}, no such proportional relationship was observed on the logarithmic plot. In addition, a large error bar appeared in the higher velocity region, because heterogeneously colored patterns were observed in the Hertzian contact circle, as shown in Figure 4a. Insufficient fluid is entrained into the conjunction area at high sliding velocities, resulting in a thinner gap. One possible reason for the color variation in the conjunction circle is a variation in the thickness of the fluid film as a result of elastic deformation of the surface and the Hertzian pressure distribution at the inlet region, the center of the conjunction circle, and off toward one side. Actually, the profile of the gap at 10^{-2} m·s^{-1} in Figure 5 might imply the elastohydrodynamic deformation. However, we should carefully consider another possibility in this experiment. Another reason might be a heterogeneous distribution of the refractive index of the thin film of fluid caused by changes in the polymer concentration.

In general, the central film thickness (H_c) of the EHL can be estimated from point-contact theory by using the following equations:

$$H_c = 7.32U^{0.64}W^{-0.22}\{1 - 0.72\exp(-0.28k)\} \quad (3)$$

$$U = \frac{\eta_0 u}{ER} \quad (4)$$

$$W = \frac{F}{ER^2} \quad (5)$$

where U, W, and k are the dimensionless speed parameter, dimensionless load parameter, and ellipticity parameter (k = 1.03), respectively. U was determined from the viscosity (η_0), the sliding velocity (u), the elastic modulus of the glass disk (E = 76.5 GPa), and the radius of curvature of the lens (R = 10.38 mm). W was determined from the normal applied load (F), E,

and R. When the zero-shear viscosity of pure water (1.0 mPa·s) was used as a value for η_0, H_c was significantly less than a few nanometers, even at $u = 10^{-1}$ m·s^{-1}, as shown in line *L4* in Figure 6b, indicating that it is hard to obtain a stable lubrication layer with pure water due to its low viscosity.

The zero-shear viscosities of 15 and 40 wt % aqueous solutions of PMTAC, measured by using a rotational rheometer at 298 K, were 8.01×10^2 and 2.42×10^4 mPa·s, respectively. Samples of free PMTAC formed simultaneously with the polymer brush were used in measuring these viscosities. If the value of η_0 is assumed to be similar to the zero-shear viscosity of a 15 wt % aqueous solution of PMTAC, the theoretical value of H_c would be expected to show a dependence on the velocity similar to line *L3* in Figure 6b. More interestingly, the experimentally observed gap determined by SLIM at $u = 2 \times 10^{-4}$ to 1×10^{-2} m·s^{-1} almost overlapped line *L2*, which represents the theoretical value of H_c calculated from the viscosity of a 40 wt % aqueous PMTAC solution. These results indicated that the swollen polymer brush in water plays a role similar to that of a viscous lubricant in assisting hydrodynamic lubrication.

The polymer concentration at the friction interface can be estimated from the graft density of the brush. The graft density σ of the PMTAC brush was determined to be 0.20 chains nm^{-2} from the M_n of the brush and its dry thickness (L_d, nm) by using eq 6:[42]

$$\sigma = (L_d d N_A / M_n) \times 10^{-21} \quad (6)$$

where d is the bulk density of the polymer (g·cm^{-3}), and N_A is Avogadro's number. In comparison with the air-dried state, PMTAC brushes in water form swollen and relatively stretched chain structures because of the high osmotic pressure. We previously measured the swollen thickness (L_e) of another batch of PMTAC brushes on a flat substrate surface by neutron reflectivity measurement.[46,47] A PMTAC brush that was 32 nm thick in the dry state was approximately 80 nm thick when swollen in water. Therefore, the value of L_e for the PMTAC brush in this work (L_d = 170 nm) would be 425 nm on the basis of simple assumptions. If σ chains of polymer are present in a volume of $L_e \times 1 \times 1$ nm^3 near the surface of the substrate, the polymer concentration (C_p) can calculated from eq 7 to be 0.58 g·cm^{-3}, which is an extremely high concentration.

$$C_p = (\sigma M_n / N_A L_e) \times 10^{21} \quad (7)$$

The presence of this extraordinary high value of C_p provides a reasonable explanation for the formation of a viscous lubrication layer at the friction interface. As previously mentioned, the observed gap was almost the same as the thickness of the theoretical lubrication layer corresponding to a 40 wt % aqueous PMTAC solution. This approximation implies that the swollen brush layer in water is capable of behaving as a highly viscous lubricant to produce stable hydrodynamic lubrication. However, we should note that this mechanism differs from that of a classical EHL system. The hydrodynamic lubrication layer in this study was formed on a water-swollen brush layer immobilized on a solid substrate. In other words, the polymer brush-enhanced the formation of an EHL system in water.

CONCLUSIONS

We investigated the water-lubrication behavior of an ion-containing PMTAC brush on a Cr−SiO_2-coated glass disk by in situ observations on a double-spacer-layer ultra-thin-film interferometry to measure the thickness of the aqueous lubrication layer at the interface between the brush and a spherical glass lens. On increasing the friction velocity from 10^{-5} to 10^{-1} m·s^{-1}, the gap between the brush-modified disk and a spherical glass lens increased significantly to 130 nm at 2×10^{-2} m·s^{-1}, and the friction coefficient simultaneously decreased to 0.01−0.02, indicating the formation of a fluid lubrication layer on the surface of the polyelectrolyte brush. A change in the interference color with friction velocity was observed only on the polyelectrolyte brush-coated substrates in water, and not on bare glass. This is a very interesting phenomenon because an artificial hydrophilic polymer brush in water forms a hydrodynamic lubrication layer even at a relatively slow friction velocity in the range 10^{-2} to 10^{-1} m·s^{-1}, reducing the friction coefficient. Therefore, this lubrication mechanism is different from that of conventional EHL, and is consequently named the "polymer brush-enhanced EHL system". The second objective of this study is the measurement of the fluid lubrication layer at symmetric interface using a brush-bound substrate and a brush-bound lens under wet condition by the interferometry.

AUTHOR INFORMATION

Corresponding Author

*Atsushi Takahara. E-mail: takahara@cstf.kyushu-u.ac.jp.

Notes

The authors declare no competing financial interest.

REFERENCES

(1) Rühe, J. Polymer Brushes On the Way to Tailor-Made Surfaces. In *Polymer Brushes: Synthesis, Characterization, Applications*; Advincula, R. C., Brittain, W. J., Caster, K. C., Rühe, J., Eds.; Wiley VCH, Weinheim, Germany, 2004; pp 1−31.

(2) Tsujii, Y.; Ohno, K.; Yamamoto, S.; Goto, A.; Fukuda, T. Structure and Properties of High-Density Polymer Brushes Prepared by Surface-Initiated Living Radical Polymerization. *Adv. Polym. Sci.* **2006**, *197*, 1−45.

(3) Klein, J. Shear, Friction, and Lubrication Forces Between Polymer-bearing Surfaces. *Annu. Rev. Mater. Sci.* **1996**, *26*, 581−612.

(4) Klein, J. Interactions, Friction and Lubrication Between Polymer-bearing Surfaces. In *Fundamentals of tribology and bridging the gap between the macro- and micro/nanoscales*; Bhushan, B. Ed.; Kluwer Academic Publishers, Dordrecht, The Netherlands, 2001; pp 177−198.

(5) Klein, J.; Perahia, D.; Warburg, S. Forces Between Polymer-bearing Surfaces Undergoing Shear. *Nature* **1991**, *352*, 143−145.

(6) Klein, J.; Kumacheva, E.; Mahalu, D.; Perahia, D.; Fetters, L. J. Reduction of Frictional Forces between Solid Surfaces bearing Polymers Brushes. *Nature* **1994**, *370*, 634−636.

(7) Kampf, N.; Gohy, J.-F.; Jérôme, R.; Klein, J. Normal and Shear Forces between a Polyelectrolyte Brush and a Solid Surface. *J. Polym. Sci., Part B: Polym. Phys.* **2005**, *43*, 193−204.

(8) Raviv, U.; Giasson, S.; Kamph, N.; Gohy, J.-F.; Jérôme, R.; Klein, J. Lubrication by Charged Polymers. *Nature* **2003**, *425*, 163−165.

(9) Nomura, A.; Okayasu, K.; Ohono, K.; Fukuda, T.; Tsujii, Y. Lubrication Mechanism of Concentrated Polymer Brushes in Solvents: Effect of Solvent Quality and Thereby Swelling State. *Macromolecules* **2011**, *44*, 5013−5019.

(10) Ruhe, J.; Ballauff, M.; Biesalski, M.; Dziezok, P.; Gröhn, F.; Johannsmann, D.; Houbenov, N.; Hugenberg, N.; Konradi, R.; Minko, S.; Motornov, M.; Netz, R. R.; Schmidt, M.; Seidel, C.; Stamm, M.; Stephan, T.; Usov, D.; Zhang, H. Polyelectrolyte Brushes. *Adv. Polym. Sci.* **2004**, *165*, 79−150.

(11) Luzinov, I.; Minko, S.; Tsukruk, V. V. Adaptive and Responsive Surfaces Through Controlled Reorganization of Interfacial Polymer Layers. *Prog. Polym. Sci.* **2004**, *29*, 635−698.
(12) Miklavic, S. J.; Marčelja, S. Interaction of Surfaces Carrying Grafted Polyelectrolytes. *J. Phys. Chem.* **1988**, *92*, 6718−6722.
(13) Klein, J.; Raviv, U.; Perkin, S.; Kampf, N.; Chai, L.; Giasson, S. Fluidity of Water and of Hydrated Ions Confined between Solid Surfaces to Molecularly Thin Films. *J. Phys.: Condens. Matter* **2004**, *16*, S5437−448.
(14) Raviv, U.; Klein, J. Fluidity of Bound Hydration Layers. *Science* **2002**, *297*, 1540−1543.
(15) Israels, R.; Leermakers, F. A. M.; Fleer, G. J.; Zhulina, E. B. Charged Polymeric Brushes: Structure and Scaling Relations. *Macromolecules* **1994**, *27*, 3249−3261.
(16) Lyatskaya, Y. V.; Leermakers, F. A. M.; Fleer, G. J.; Zhulina, E. B.; Birshtein, T. M. Analytical Self-Consistent-Field Model of Weak Polyacid Brushes. *Macromolecules* **1995**, *28*, 3562−3569.
(17) Zhulina, E. B.; Wolterink, J. K.; Borisov, O. V. Screening Effects in a Polyelectrolyte Brush: Self-Consistent-Field Theory. *Macromolecules* **2000**, *33*, 4945−4953.
(18) Pincus, P. Colloid Stabilization with Grafted Polyelectrolytes. *Macromolecules* **1991**, *24*, 2912−2919.
(19) Ross, R. S.; Pincus, P. The Polyelectrolyte Brush: Poor Solvent. *Macromolecules* **1992**, *25*, 2177−2183.
(20) Pryamitsyn, V. A.; Leermakers, F. A. M.; Fleer, G. J.; Zhulina, E. B. Theory of the Collapse of the Polyelectrolyte Brush. *Macromolecules* **1996**, *29*, 8260−8270.
(21) Taunton, H. J.; Toprakcioglu, C.; Fetters, L. J.; Klein, J. Forces between Surfaces Bearing Terminally Anchored Polymer Chains in Good Solvents. *Nature* **1988**, *332*, 712−714.
(22) Eiser, E.; Klein, J.; Witten, T. A.; Fetters, L. J. Shear of Telechelic Brushes. *Phys. Rev. Lett.* **1999**, *82*, 5076−5079.
(23) Hayashi, S.; Abe, T.; Higashi, N.; Niwa, M.; Kurihara, K. Polyelectrolyte Brush Layers Studied by Surface Forces Measurement: Dependence on pH and Salt Concentrations and Scaling. *Langmuir* **2002**, *18*, 3932−3944.
(24) Kampf, N.; Ben-Yaakov, D.; Andelman, D.; Safran, S. A.; Klein, J. Direct Measurement of Sub-Debye-Length Attraction between Oppositely Charged Surfaces. *Phys. Rev. Lett.* **2009**, *103*, 118304.
(25) Kelley, T. W.; Shorr, P. A.; Kristin, D. J.; Tirrell, M.; Frisbie, C. D. Direct Force Measurements at Polymer Brush Surfaces by Atomic Force Microscopy. *Macromolecules* **1998**, *31*, 4297−4300.
(26) Torolin, V.; Ranetcaia, N.; Hamciuc, V.; Shore, N.; Dörr, N.; Ibanescu, C.; Simionescu, B. C.; Hrabagiu, V. Influence of Ionic Structure on Tribological Properties of Poly(dimethylsiloxane-alkylene oxide) Graft Copolymers. *Tribol. Int.* **2013**, *67*, 1−10.
(27) Hsiao, E.; Kim, D.; Kim, S. H. Effects of Ionic Side Groups Attached to Polydimethylsiloxanes on Lubrication of Silicon Oxide Surfaces. *Langmuir* **2009**, *25*, 9814−9823.
(28) Hsiao, E.; Bradley, L. C.; Kim, S. H. Improved Substrate Protection and Self-Healing of Boundary Lubrication Film Consisting of Polydimethylsiloxane with Cationic Side Groups. *Tribol. Lett.* **2011**, *41*, 33−40.
(29) Kobayashi, M.; Terayama, Y.; Hosaka, N.; Kaido, M.; Suzuki, A.; Yamada, N.; Torikai, N.; Ishihara, K.; Takahara, A. Friction Behavior of High-Density Poly(2-methacryloyloxyethyl phosphorylcholine) Brush in Aqueous Media. *Soft Matter* **2007**, *3*, 740−746.
(30) Kobayashi, M.; Takahara, A. Tribological Properties of Hydrophilic Polymer Brushes Under Wet Conditions. *Chem. Records* **2010**, *10*, 208−216.
(31) Ishikawa, T.; Kobayashi, M.; Takahara, A. Macroscopic Frictional Properties of Poly(1-(2-methacryloyloxy)ethyl-3-butyl Imidazolium Bis(trifluoromethanesulfonyl)imide) Brush Surfaces in an Ionic Liquid. *ACS Appl. Mater. Interfaces* **2010**, *2*, 1120−1128.
(32) Sakata, H.; Kobayashi, M.; Otsuka, H.; Takahara, A. Tribological Properties of Poly(methyl methacrylate) Brushes Prepared by Surface-Initiated Atom Transfer Radical Polymerization. *Polym. J.* **2005**, *37*, 767−775.
(33) Kobayashi, M.; Takahara, A. Synthesis and Frictional Properties of Poly(2,3-dihydroxypropyl methacrylate) Brush Prepared by Surface-Initiated Atom Transfer Radical Polymerization. *Chem. Lett.* **2005**, *34*, 1582−1583.
(34) Kobayashi, M.; Ishida, H.; Kaido, M.; Suzuki, A. Takahara, A. Tribological Behavior of Ionic Polymer Brushes in Aqueous Environment. In *Surfactants in Tribology Volume 3*; Biresaw, G., Mittal, K. L., Eds.; CRC Press: Boca Raton, FL., 2013; pp 75−92.
(35) Kobayashi, M.; Wang, Z.; Matsuda, Y.; Kaido, M. Suzuki, A.; Takahara, A. Tribological Behavior of Polymer Brush Prepared by the "Grafting-from" Method. In *Polymer Tribology*, Kumar, S. S., Ed.; Imperial College Press: London, 2009; pp 582−602.
(36) Spikes, H. A. Boundary Lubrication and Boundary Films. In *Thin Films in Tribology*; Dowson, D., Talor, C. M., Childs, T. H. C., Godet, M., Dalmz, G., Eds.; Elsevier: New York, 1993; pp 331−346.
(37) Dowson, D.; Higginson, G. R.; Archard, J. *Elastohydrodynamic Lubrication, SI ed.*; Pergamon Press, Oxford, U. K., 1977.
(38) Bielecki, R. M.; Crobu, M.; Spencer, N. D. Polymer-Brush Lubrication in Oil: Sliding Beyond the Stribeck Curve. *Tribol. Lett.* **2013**, *49*, 263−272.
(39) Gohar, R.; Carmeron, A. Optical Measurement of Oil Film Thickness under Elasto-hydrodynamic Lubrication. *Nature* **1963**, *200*, 458−459.
(40) Fu, Z.; Guo, F.; Wong, P. L. Theoretical Study on the Interferometry of Thin EHL Film Measurement. *Tribol. Lett.* **2008**, *31*, 57−65.
(41) Sugimura, J.; Jones, W. R.; Spikes, H. A. EHD Film Thickness in Non-Steady State Contacts. *ASME J. Tribol.* **1998**, *120*, 442−452.
(42) Kobayashi, M.; Terada, M.; Terayama, Y.; Kikuchi, M.; Takahara, A. Direct Synthesis of Well-Defined Poly[{2-(methacryloyloxy)ethyl}trimethylammonium chloride] Brush via Surface-Initiated Atom Transfer Radical Polymerization in Fluoroalcohol. *Macromolecules* **2010**, *43*, 8408−8415.
(43) When a glass ball (A) contacts on a flat silicon wafer (B) under a normal load P (0.49 N), the following equations are used

$$\frac{1}{E} = \frac{1-\upsilon_A^2}{E_A} + \frac{1-\upsilon_B{}^2}{E_B}$$

$$a = \left(\frac{3PR_A}{4E}\right)^{1/3}$$

where E_A (7.16×10^{10} Pa) and E_B (1.30×10^{11} Pa) are Young's modulus of glass and silicon wafer, υ_A (0.23) and υ_B (0.28) are Poisson's ratio, R_A is curvature radius (5.00×10^{-3} m) of glass ball, and a (m) is radius of a circle formed by contact of ball and flat plate. Normal pressure was determined by P divided by contact area (πa^2). In the case of interferometry setup, Young's modulus and Poisson's ratio for BK7 were 7.16×10^{10} Pa and 0.22, respectively. Curvature radius of glass lens was 10.38×10^{-3} m.
(44) Cann, P. M.; Hutchinson, J.; Spikes, H. A. The Development of a Spacer Layer Imaging Method (SLIM) for Mapping Elastohydrodynamic Contacts. *Tribol. Trans.* **1996**, *39*, 915−921.
(45) Hamrock, B. J.; Dowson, D. Isothermal Elastohydrodynamic Lubrication of Point Contacts Part II − Fully Flooded Results. *ASME J. Lubr. Technol. Trans.* **1977**, *99*, 264−276.
(46) Mitamura, K.; Yamada, N. L.; Sagehashi, H.; Torikai, N.; Arita, H.; Terada, M.; Kobayashi, M.; Sato, S.; Seto, H.; Goko, S.; Furusaka, M.; Oda, T.; Hino, M.; Jinnai, H.; Takahara, A. Novel Neutron Reflectometer SOFIA at J-PARC/MLF for in-Situ Soft-Interface Characterization. *Polym. J.* **2013**, *45*, 100−108.
(47) Kobayashi, M.; Takahara, A. Neutron Reflectivity Study of the Swollen Structure of Polyzwitterion and Polyeletrolyte Brushes in Aqueous Solution. *J. Biomat. Sci. Polym. Ed.* **2014**, *25*, 1673−1686.